Downloaded from http://sp.lyellcollection.org/ at Carleton University Library on June 13, 2015

Coelobiontic communities in neptunian fissures of synsedimentary tectonic origin in Permian reef, southern Urals, Russia

EMMANUELLE VENNIN

Biogéosciences, Université de Bourgogne, 21000 Dijon, France
(e-mail: emmanuelle.vennin@u-bourgogne.fr)

Abstract: Sedimentary dykes in the Permian reef complexes of the Russian platform are well preserved and important in providing information about reef growth, the reef biota and, particularly, cavity-dwelling organisms and sediment sources. Two main fissure assemblages are recognized with N80° and N170° (late Asselian–early Sakmarian) and N130°–140° and N60° (Sakmarian–Artinskian) orientations. These contemporaneous orthogonal dyke sets present orientations corresponding to the regional tectonic fabric and a tectonic origin for fracturing associated with the foreland basin development. The largest dykes record eight lithofacies and several stages of fracture opening. Stromatoids and centimetre-thick deposits of peloidal grainstones–packstones (thromboids), which form *in situ* within microbial laminae on the fissure walls, preceded filling by skeletal and terrigenous sediments. The fissures contain a well-preserved biota similar to the Lower Permian cavity-dwelling organisms observed within the reef. The coelobiontic habitat was episodically enlarged by successive synsedimentary fracturing episodes reflecting several phases of encrustation and infill of recurrent lithofacies. The pioneer microbialites grew when nothing else was deposited in the fissures immediately after fracturing. Gastropods and ostracods occur as dense clusters, probably indicating *in situ* growth, or are considered as reworked material from the subsurface. Others organisms, such as crinoids, bryozoans, *Tubiphytes*, conodonts, brachiopods, ammonoids and spiculate sponges, are also found within fractures as reworked shells and skeletons, indicating that they were washed in from the overlying sea floor. The biota in the dykes is mainly represented by the dweller guilds living on the reef surface, whereas members of the binding and framebuilding guilds are poorly represented. The dykes formed during reef development and the last stage of argillaceous wackestone sedimentation within the fractures is related to a major flooding event corresponding to upper Artinskian drowning of the Russian platform. Biostratigraphically significant fossils in the dykes date the ages of the host rock and of the fissure formation and filling from late Asselian to upper Artinskian. The Tratau reef thus provides an instructive example of the interaction between carbonate accumulation and tectonic events.

Carbonate buildups are characteristic components of the Carboniferous–Permian strata cropping out in the southern Urals, or present in the adjacent subsurface. They proliferated in a transitional area between the eastern margin of the Russian platform and the preduralian foredeep basin (Fig. 1a, b). This platform, flanking an eastern subduction complex, is characterized by the common reef occurrence during late Carboniferous–early Permian time. Biostratigraphic data, mainly based on the study of fusulinids and ammonoids (Rauser-Chernoussova 1951; Vissarionova 1975; Chuvashov *et al.* 1996; Lys & Moreau 1989 unpublished) and the location of reef belts, indicate a westward migration of the reef depocentres (Chuvashov 1983) away from the megasuture, with a maximum development during the Asselian–Sakmarian.

The Sterlitamak area in the southern Urals (Russia) records the largest reefs. These appear as isolated reefs in scattered localities across a north–south-trending area (Fig. 1b). The overall facies and thickness change along linear trends (Rauser-Chernoussova 1951), and their spotty distribution, in conjunction with evidence of synsedimentary faulting, suggest that their origin and growth were dictated by synsedimentary tectonism that also controlled local bathymetry and hydrodynamic conditions (Vennin *et al.* 2002). Neptunian dykes provide a significant key to the regional history of vertical movement relative to sea level (tectonic and/or eustatic).

Neptunian dykes are sedimentary dykes in which the filling sediments are derived from above (i.e. the surface), in contrast to some sedimentary dykes with fill injected from below (Winterer & Sarti 1994). Neptunian dykes exhibit a complex infilling including loose skeletal material, peloidal packstones–grainstones, mudstones and wackestones, microbialites, breccias and argillaceous wackestones. They provide a site

From: ÁLVARO, J. J., ARETZ, M., BOULVAIN, F., MUNNECKE, A., VACHARD, D. & VENNIN, E. (eds) 2007. *Palaeozoic Reefs and Bioaccumulations: Climatic and Evolutionary Controls.* Geological Society, London, Special Publications, **275**, 211–227. 0305-8719/07/$15.00 © The Geological Society of London.

Downloaded from http://sp.lyellcollection.org/ at Carleton University Library on June 13, 2015

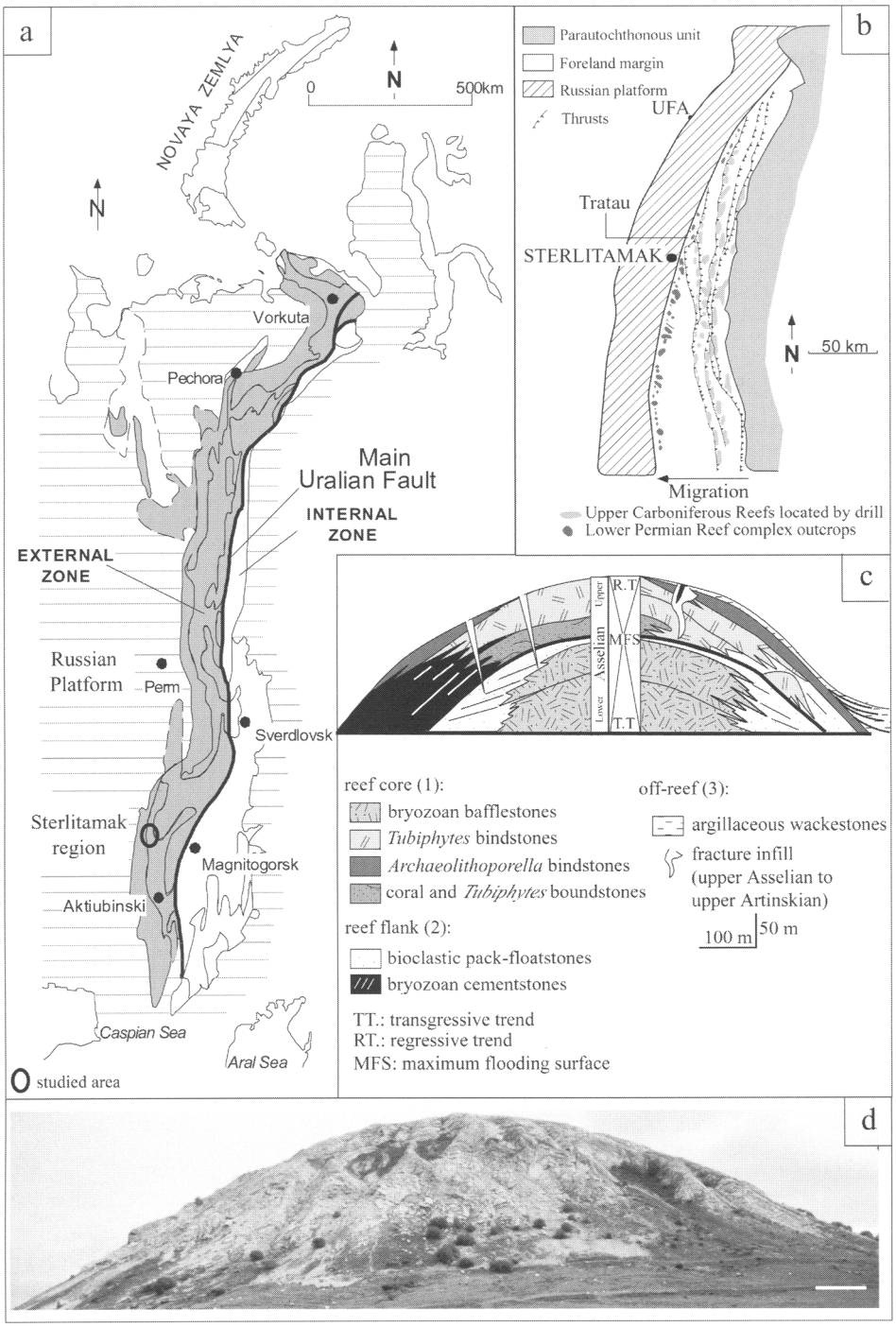


Fig. 1. (**a**) Regional map depicting main geological characteristics of the Urals Mountains. (**b**) Map showing the westward migration of reefs in the Sterlitamak area (central Urals). (**c**) Schematic sedimentary architecture and sequence framework of the Tratau reef. It shows a major transgressive–regressive sequence. (**d**) Tratau reef near Sterlitamak. The differential weathering of Permian basin-fill that covered the reef reveals the depositional architecture and a palaeo-relief of 250 m; Scale = 100 m.

Downloaded from http://sp.lyellcollection.org/ at Carleton University Library on June 13, 2015

where organisms could be preserved away from the destructive taphonomic processes active on the sea floor and the removal of sediments by erosion. Neptunian dykes give information about platform growth, sediment sources and the biota that were present on the platform. Early Lower Permian fracture-dwelling organisms are recorded within the fissure in Permian reefs in the Sterlitamak area. These fractures offer a record of new-eroded surface sedimentation. Fractures were episodically enlarged by synsedimentary tectonic fracturing reflecting several phases of infill of recurrent facies, and intraclasts.

The knowledge of the diagenetic processes undergone by the reef is essential for an understanding of: (i) the timing of mud lithification and the preservation of high angles in the flanks; (ii) the origin of distinct fabrics, particularly related to cavity systems and synsedimentary fissures; (iii) the absence of both compaction and plastic deformation processes; and (iv) the marine origin of calcite cements (according to their isotopic signature). In addition, geochemical data from void-filling cements and documentation of the burial history of the rocks provide details regarding their depositional environments. These reefs have received considerable attention because subsurface ones form important reservoirs in the Ishimbaevo fields.

The purpose of this paper is to: (1) demonstrate the synsedimentary tectonic signature reflected in one of the most significant reefs of the Sterlitamak area; (2) analyse the stratigraphic and facies distribution, geometry and diagenetic features of this reef; (3) determine how, where and when neptunian dykes developed; and (4) illustrate the stepwise colonization displayed by Early Permian benthic organisms (mainly microbial communities and gastropods) in sedimentary fissures.

Geological setting

Tratau Hill is located 10 km SE of Sterlitamak village and is one of the better exposed Upper Carboniferous–Lower Permian carbonate reefs cropping out in the Sterlitamak–Ishimbaevo area of the southern Urals. During this time Laurasia and the Pangean supercontinent were assembled and reefal accumulations are restricted to intracontinental land masses and neighbouring foredeeps. The Uralian foreland basin is an asymmetric structure formed by flexure of the European craton in response to tectonic loading by the Uralian Orogen (Zonenshain *et al.* 1984). The Tratau reef belongs to the sedimentary cover of the east European craton, and is located at the margin between the western Russian platform and the eastern preduralian foreland basin. It crops out in the external tectonostratigraphic unit of the Urals, separated from the internal one by the main Uralian fault (Fig. 1a). In the preduralian basin, Uralian orogenesis produced a thick flysch that prograded across the axis of the basin rapidly to the west. During the Carboniferous–Permian the Russian platform recorded several episodes of backstepping that resulted in a shrinking of the carbonate shelf area and in gradual shifting of the shelf margin westwards (Fig. 1b) (Chuvashov 1983; Vennin *et al.* 2002). Following margin backstepping, reefs formed a major belt mainly owing to differential subsidence in the whole region.

A regional study of reefs shows the continuity of reef formation through the Sakmarian and the end of the carbonate productivity in the Burservskian (early Artinskian). During Asselian times there was widespread development of isolated reefs (Vennin *et al.* 2002). The uppermost Asselian is a time of subaerial exposure evidenced throughout the East European platform (Aisenberg *et al.* 1983). Whereas only three stratigraphic units have been observed in the Tratau reef for the Lower Permian, five units are identified in the Shaktau reef located 15 km to the north (Vennin *et al.* 2002). The two missing units in the Tratau reef correspond, respectively, to the lower Sakmarian deposits composed mainly of *Palaeoaplysina* and coral biostromes embedded in bioclastic packstones–grainstones, and to the upper Sakmarian deposits with fusulinid grainstones and small *Palaeoaplysina* biostromes and bryozoan bafflestones. The top of the Sakmarian is characterized by a significant karst surface on the platform (Vennin *et al.* 2002; Zempolich *et al.* 2002). Finally, the platform margin where reefs developed was progressively drowned, culminating with a flooding of the platform and the deposition of upper Artinskian argillaceous wackestones (dated by Gerasimov 1940; Ruzhencev 1956; Chuvashov 1984) overlaying an important erosional surface of Early Artinskian age (Rauser-Chernoussova 1951). This erosion corresponds to the Burservskian erosion recognized by Chuvashov *et al.* (1996). The late Artinskian *Cladoconus*–argillaceous wackestones coincide with a widespread transgressive trend of eustatic origin (Sloss 1972; Ross & Ross 1990). Differences in regional sedimentation between reefal areas during late Asselian–Artinskian are related to a breakdown of the platform in the area of the isolated palaeohighs where reefs were initiated (Korolyuk 1985; Vennin *et al.* 2002).

Downloaded from http://sp.lyellcollection.org/ at Carleton University Library on June 13, 2015

The Tratau reef is classified as a Duvansk-type buildup (Nalivkin 1950). The exposed dimensions of the reef are 270 m in height and about 1 km in diameter (Fig. 1c, d), but the real thickness of this buildup is about 400 m according to borehole data. In the southern Urals exposed reefs retain their palaeodepositional relationship (i.e. relief) with respect to the basin floor. The Tratau Hill shows a hemispheric–conical morphology owing to the preservation of flanks inclined up to 40° (Fig. 1c, d). It overlies Gzhelian carbonate strata (Shamov 1984), and is covered by upper Artinskian argillaceous wackestones as seen on the northern part of the reef.

Biostratigraphically significant fossils (conodonts, ammonoids, foraminifers) in the dykes date the age of the host rock and fissure formation and infill. Sediments infilling fractures are late Asselian–upper Artinskian (Chuvashov *et al.* 1996).

Reef complex anatomy

Three distinct stratigraphic units can be differentiated in the Tratau reef (Fig. 1c). The two first units are separated by a sharp facies boundary identified as a maximum flooding surface, just on the top of the basal unit. This is a thin and continuous layer, 20 cm thick, made up of wackestones and packstones rich in ammonoids, orthoceratids, bryozoans, brachiopods, bivalves, crinoids, gastropods, foraminifers and problematic algae. The third unit is separated from the second one by an important erosive surface (sequence boundary).

(i) The basal unit (*Sphaeroschwagerina moelleri–Schwagerina fecunda* Zone; lower *Schwagerina* Horizon) is about 100 m thick. Its core consists of massive bryozoan bafflestones and coral and bryozoan wackestones. Complete bryozoans (Fenestellidae and encrusting forms), *Tubiphytes* and corals are preserved in life position, locally encrusted by *Archaeolithoporella*, and associated with crinoids, brachiopods, *Diplosphaerina*, foraminifers and ostracods.

The flanks are composed of bedded bryozoan and coral floatstones. Bryozoans, corals, *Tubiphytes*, sponge spicules and ammonoids are the predominant bioclasts in these flanks; foraminifers, crinoids, brachiopods, *Palaeoaplysina*, bivalves and ostracods are disseminated in the matrix.

(ii) The second unit (*Sphaeroschwagerina sphaerica–Schwagerina firma* Zone) also shows lateral facies changes from core to flanking areas, although the core is not well exposed. Equivalent core facies are observed in the nearly Shaktau reef situated 15 km to the south where it consists of *Tubiphytes* and *Archaeolithoporella*-rich bindstones. The flanking beds, 50 m thick, show a mosaic of facies: (a) the NW flank is composed of a vertical succession of *Tubiphytes* and bryozoans bindstones and floatstones, intraclast, coral and crinoidal floatstones, bryozoan cementstones and common *Archaeolithoporella* bindstones at the top; (b) the southern flank is characterized by *Tubiphytes* floatstones alternating with bryozoan cementstones, while its uppermost part shows *Archaeolithoporella* bindstones; (c) the SE flank consists of *Palaeoaplysina* floatstones, *Tubiphytes* and *Archaeolithoporella* bindstones; and (d) the northern flank is composed of *Archaeolithoporella* bindstones overlain by Artinskian argillaceous wackestones and cherts.

(iii) The third unit consists of Artinskian argillaceous wackestones onlapping Asselian and, locally, Sakmarian deposits. Argillaceous wackestones crop out on the northern flank of the reef and fill synsedimentary fractures.

In summary, the Tratau reef is composed mainly of non-framework facies characterized by: (i) dominantly baffling organisms (bryozoans); (ii) the occurrence of binding and encrusting organisms (*Tubiphytes*, *Archaeolithoporella* and foraminifers); and (iii) a diverse dwelling fauna including corals, palaeoaplysinids, gastropods, bivalves, etc. Binding processes by the microbial organisms and various encrusting organisms, in conjunction with sediment baffling by bryozoans, are considered to have played a sediment-stabilizing and binding role rather than a frame-building one.

Whereas the core is envisaged as the site of carbonate production and entrapment, the bedded nature of the flank facies indicates local downslope transport and lateral accretion of sediment derived from the core. The intraclasts are composed of material identical to that of the core, relocated by storm- and/or gravity-induced transport. The high dipping angle (up to 40°) suggests that the flanks have somehow been stabilized during reef growth by cementation and encrustation.

Diagenetic processes

A complex diagenetic history is observed in the Tratau reef and comprises seven successive episodes: (i) deposition of homogeneous and peloidal–clotted micrite; (ii) dissolution; (iii) precipitation of multiple phases of radial fibrous cements; (iv) precipitation of cements alternating

Downloaded from http://sp.lyellcollection.org/ at Carleton University Library on June 13, 2015

with peloidal matrix; (v) second phase of dissolution; (vi) precipitation of a second generation of radial fibrous cements; and (vii) infill of fractures. The occurrence of massive cementstones in reef-slope and platform-margin settings suggests that cements were a fairly common component in reef flanks. These Lower Permian reefs contain fibrous magnesium calcite cements (high Mg contents) low in Sr (Wahlman & Konovalova 2002; Zempolich *et al.* 2002).

The carbonate mud displays two textures that are present at all stages of reef growth: (i) homogeneous micrite is present in the reef core strata, in cavities and fractures; (ii) peloids are spherical ('structure grumeleuse'), up to 50–100 μm in diameter, and present in the flanking strata, in cavities and fractures. In cavities and fractures, peloids are interstratificated with bands of radial fibrous calcite cements, forming planar (0.5–5 mm thick) to dome-shaped structures (2–5 mm high). Under cathodoluminescence, the micrite presents a homogeneous dull luminescence. Peloidal sediment is thought to represent microbially induced marine cementation that contributed significantly to the cohesiveness of many reefs. Micrites are a quantitatively important component of the Tratau reef core (up to 40%). The recognition of producing organisms is difficult but the presence of micritic laminae may be assigned to microbialites (Kirkland *et al.* 1998; Weidlich & Fagerstrom 1999; Weidlich 2002). The isolated position of the Tratau reef flanked by terrigenous sediment (argillaceous wackestones) prevented mud input from the platform, whereas the presence of clotted and peloidal micrites, and fine microbial laminae, argue for microbial activity (automicrite: Reitner *et al.* 1995). The micrite in phylloid algal mounds as well as in reefs is interpreted as the result of biological *in situ* production (Guo & Riding 1992; Kirkland *et al.* 1998). Microbes played a significant role in reef building (Riding, 2000, 2002) for sediment stabilization, sediment binding and precipitation. In the Tratau reef, carbonate mud seems to have resulted from the trapping of fine particles, *in situ* calcification of microbial cells, and disintegration of *Archaeolithoporella* and bioerosion of bioclasts.

Early–late dissolution episodes correspond, respectively, to primary pore types and secondary ones. Early dissolution created mouldic and inter- and intraparticle pores, fenestrae and stromatactis-like systems. Late dissolution episodes enlarged primary voids, which acted as access routes for the aggressive fluids, and produced large voids, vugs and discontinuities in fissures and fractures.

Stromatactis cavities identical to the classical Belgian forms (Bourque & Boulvain 1993) occur in both core and flank facies of the first two units (Figs 2 & 3). The size of these cavities ranges from centimetres to decimetres, and their length/height ratio ranges from 1 to 2.5. The orientation of stromatactis varies from horizontal in the core (Fig. 3a) to up to 40° inclined in flanking beds (Fig. 3b). Stromatactis cavities can be interconnected by synsedimentary fissures (up to 0.5 cm wide) filled by fibrous calcite cements (Fig. 3c). The resulting cavity networks exhibit a more complex filling by internal sediments and centripetally oriented radial fibrous calcite (of marine origin) and botryoidal calcite (Fig. 3d). The various attributes of stromatactis show a direct relationship between complex filling of cavities and type of enclosing beds, and size and shape of cavities related to enclosing beds (Fig. 2). The largest cavities display four types of infill (Fig. 2): (i) cements (botryoidal and radial fibrous calcite cements) frequently associated with microbialites and peloidal grainstones; (ii) micrite with bioclasts; (iii) microdolomite; and (iv) argillaceous wackestones. Contacts between upper walls and cavity-filling cement are invariably sharp. Stromatactis in the Tratau reef has not affected surrounding bioclasts, and radial fibrous calcite has not replaced matrix indicating that they were true cavities. These obervations suggest formation by fluid escape after sediment collapse. Cavities may have formed as well as a result of a lateral compression resulting from gravity acting on the reef slope, a phenomenon that induced opening fractures and cavities. Stromatactis parallel to the inclined bedding of reef flank is thought to have been formed, in part, due to gravitational processes, which have been triggered by seismic activity, given the instable shelf position of reefs (Lees 1964). Perhaps decay of soft-bodied multicellular organisms (spicular sponges) could have left cavities (e.g. Bourque & Boulvain 1993).

Marine phreatic cements (Vennin 1997) comprise 50–80% of the rock fabric and are botryoidal and isopachous radial fibrous calcite in primary porosity, stromatactis cavities, solution-modified pore space and locally in the open fractures. Banding is recognized in radial fibrous cements, with five alternating dark and light layers, while eight luminescent bands are visible by cathodoluminescence. The alternating luminescent radial fibrous calcite and peloidal laminae are well expressed in stromactatis cavities. The marine origin of these cements is evidenced by stable isotope values for the radial fibrous calcite crystals that show a limited range

Downloaded from http://sp.lyellcollection.org/ at Carleton University Library on June 13, 2015

Host facies	Size		Infilling	Dip of bases	Position in reef	
	width (cm)	thick (cm)			flank	core
Bryozoan and *Tubiphytes* cementstones	1–10	1–2	cements (radiaxial, fibrous calcite), micrite, and argillaceous wackestones	20–45°	X	
Tubiphytes, bryozoan and coral baffl estones	1–100	1–50	cements (botryoidal and radial fibrous calcite) - micrite-dolomite, and argillaceous wackestones	0–3°		X
Algal, bryozoan and *Tubiphytes* bindstones	1–50	1–15	cements (botryoidal and radial fibrous calcite): dolomite, and argillaceous wackestones	0–35°	X	X
Tubiphytes, bryozoan and crinoid baffl estones	1–100	1–100	cements (rare botryoidal and radial fibrous calcite): dolomite, and argillaceous wackestones	0–20°	X	X

Fig. 2. Table showing a classification of stromatactis cavities in the Tratau reef according to their respective shape, size, infilling, measurements of the dip of bases and setting.

of variation in ^{13}C and ^{18}O values ($\delta^{18}O$ from –0.5 to –2.1‰ and $\delta^{13}C$ from 4.7 to 6.2‰). Isotopic and trace-element analyses in the Shaktau reef conducted by Zempolich *et al.* (2002) gave similar values. Radial fibrous calcite cements are non-luminescent and inclusion-rich with elevated Mg contents and low Mn and Fe contents. They are interpreted therefore to have precipitated from marine waters as primary high-Mg calcite. Early marine cementation and the binding action of encrusting microbes are the most likely factors that led to an early stabilization of the flank slopes, and early internal filling of fractures.

The origin of extensive cementstones correlated with the biota associated is suggested by Grotzinger & Knoll (1995). This association may be related to the delivery of trophic resources to slope and platform-margin settings. There is a clear correlation between the abundance of suspension-feeding and nutrient-tolerant organisms and the occurrence of marine cements (Vennin *et al.* 2002; Zempolich *et al.* 2002). The biotic and abiotic constituents need substantial quantities of organic matter and HCO_3^- to sustain growth and precipitation. These components are common in waters upwelling along continental margins (Zempolich 1993). Upwelling processes have been proposed in the Uralian foredeep margin and related to the circulation of polar currents southwards along the margin of the Russian platform, and to progressive infilling of the Urals with clastics and resedimented carbonate during the early Permian (Chuvashov 1983).

Evidence for syndepositional tectonic processes

Synsedimentary fissures and fractures, seen as neptunian dykes, are distinctive sedimentary structures of the Tratau reef. They are related to synsedimentary tectonism rather than gravitational phenomena on the reef flank.

Dyke sediments and biota

Sediment-filled fractures are common (Figs 4 & 5). The fractures sizes range from a few centimetres up to 10 m in width, and up to 500 m in length. Most are subvertical to steeply inclined. The fracture opening post-dates reef formation, and thus has the latest Asselian as maximum age. Stromatactis cavity formation must have a pre-late Asselian age because they are cut by the complex synsedimentary fractures.

Downloaded from http://sp.lyellcollection.org/ at Carleton University Library on June 13, 2015

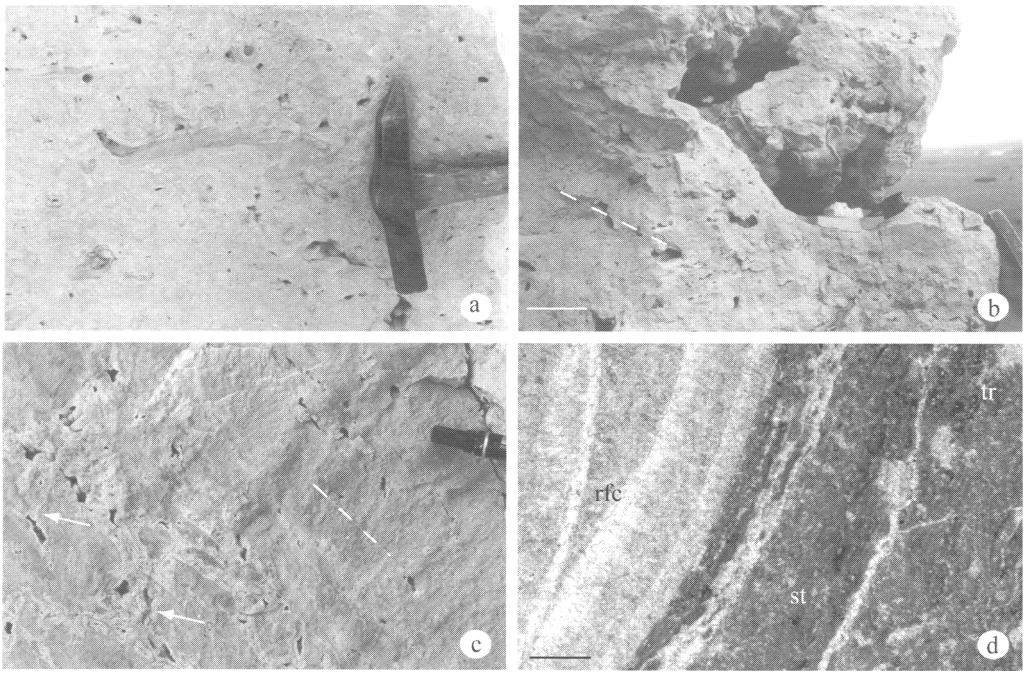


Fig. 3. (**a**) Stromatactis characterized by a complex filling composed of micritic, peloidal and clotted matrix and radial fibrous calcite cements (hammer for scale). (**b**) Horizontal stromatactis-like cavity oblique, respectively, to bedding and characterized by a complex filling: micritic matrix and botryoid developed on the cavity roof. (**c**) Stromatactis parallel to bedding (white dotted line) and fracture network (white arrow) connecting stromatactis cavities filled by radial fibrous calcite cements. (**d**) Large botryoid (rfc, radial fibrous cement) alternating with microbial laminae (st, up to 5 cm thick) covered by peloidal packstone (tr) with millimetre-thick microbial layers; scale = 250 μm.

Correctness of the age determinations depends on whether the fossils lived contemporaneously with filling or had been reworked from older sediments. Preservation of diagnostic fossils as individual specimens not micritized and without taphonomic and diagenetic transformations indicates that reworking was insignificant, as opposed to specimens found in lithoclasts.

Two successive assemblages of dykes can be identified. There orientations are: (i) N80° and N170° (late Asselian–early Sakmarian; Figs 5 & 6); and (ii) N130°–N140° and N60° (Sakmarian–Artinskian; Figs 5 and 7). Their infills exhibit a fairly uniform composition of eight lithofacies.

(i) A multiple phase of sediment layering, perpendicular or inclined to the fracture walls, dominates in the earlier assemblage (Fig. 5c, d). At least four distinct neptunian lithofacies separated by erosion surfaces are recognized in the more complete fractures, from inner to outer. The vertical lithofacies succession is represented by: (a) oolithic, peloidal and lumpy (irregular aggregates of carbonate mud) grainstones–packstones (lithofacies 4a; Fig. 6c). Laminae are variably oblique to the fissure walls and show soft-sediment folding and convolution related to water escape and liquefaction; (b) intraclastic breccias (lithofacies 7) composed of mudstone. They are assigned to early lithification fracture of muddy sediment (in agreement with syndepositional seismic activity); (c) alternating wackestones and packstones rich in ostracods and gastropods (lithofacies 4b; Fig. 6a); (d) fenestrae mudstones (lithofacies 4c; Fig. 6b). Fenestrae are parallel to the inclined stratification. Silty dolomite fills the late porosity in fenestrae below the erosive surface observed at the top of these mud-rich deposits (lithofacies 4c). Its stratification within the fenestrae is concordant with the horizontal, respectively inclined to the stratification plane; (e) the erosion surface is covered by a bioclastic packstone composed mainly of crinoids, brachiopods, conodonts and rare

Downloaded from http://sp.lyellcollection.org/ at Carleton University Library on June 13, 2015

dykes	width (m)	vertical extent (m)	lateral length (m)	Facies	Biofacies and taphonomy	Diagenesis
Type 1: N80°/N170° orientation	0.10–1	>25	5–100	Ooidal and peloidal packstones to grainstones (lithofacies 4a). Nuclei of ooids are generally micritic, cortices have a poorly-developed radial fabric. Peloids (25–100μm) are irregular, intraclasts are less common, up to 5cm in size. The facies consists of laterally lenticular to discontinuous beds	Ostracods are articulated to disarticulated. Gastropods are arranged in clusters. This fauna is otherwise absent in subsurface.	Fenestrae are filled by radial fibrous calcite cement, and dolomite filling the remaining pore space. Ooids in grainstones are surrounded by equant spar (10–30μm) to drusy sparite (related to early meteoric diagenesis). Silt-grained dolomite fills stromatactoid-like cavities near the fractures and fenestrae preserved in the fractures.
				Wackestones/packstones rich in ostracods and gastropods (lithofacies 4b) and intercalated fenestral (birdeyes) mudstones (lithofacies 4c).		
				Stromatolites and peloidal packstones to grainstones frequently encrust dyke wall (lithofacies 2 and 3).	Microbialites	Ferruginous and phosphatic crusts (lithofacies 1) Large botryoidal and radial fibrous high-Mg calcite cement associated with lithofacies 2 and 3 only.
				Bioclastic packstones composed of crinoids, bryozoans. Tubiphytes, brachiopods, bivalves, conodonts and foraminifers (lithofacies 5). Brachiopods and bivalves are articulated and matrix includes peloids and intraclasts. Bioclasts are encrusted by foraminifers.	Fossils are disarticulated and fragmented; and articulated (bivalves)	
				Marls rich in conodonts, ammonoids and ostracods (lithofacies 8).	Fossils are complete and disarticulated.	
Type 2: N130–140°/N60° orientation	0.50–10	>50	1–500	Bioclastic packstones composed of bryozoans, *Tubiphytes*, brachiopods, ostracods, foraminifers, trilobites, bivalves and echinoderms (lithofacies 6a). Grains (0.5–5mm in diameter) embedded in a micritic matrix.	Bioclasts are encrusted by foraminifers, and bryozoans are encrusted by Tubiphytes. Bioclasts are commonly fragmented.	Isopachous fibrous calcite cement surrounding bioclasts and fill pore spaces. Equant spar (10–30μm)
				Packstones rich in sponge spicules (80%), associated echinoderms, brachiopods and foraminifers (lithofacies 6b).		

Fig. 4. Table showing the characteristics of dykes including facies, biofacies, taphonomy and diagenesis.

Downloaded from http://sp.lyellcollection.org/ at Carleton University Library on June 13, 2015

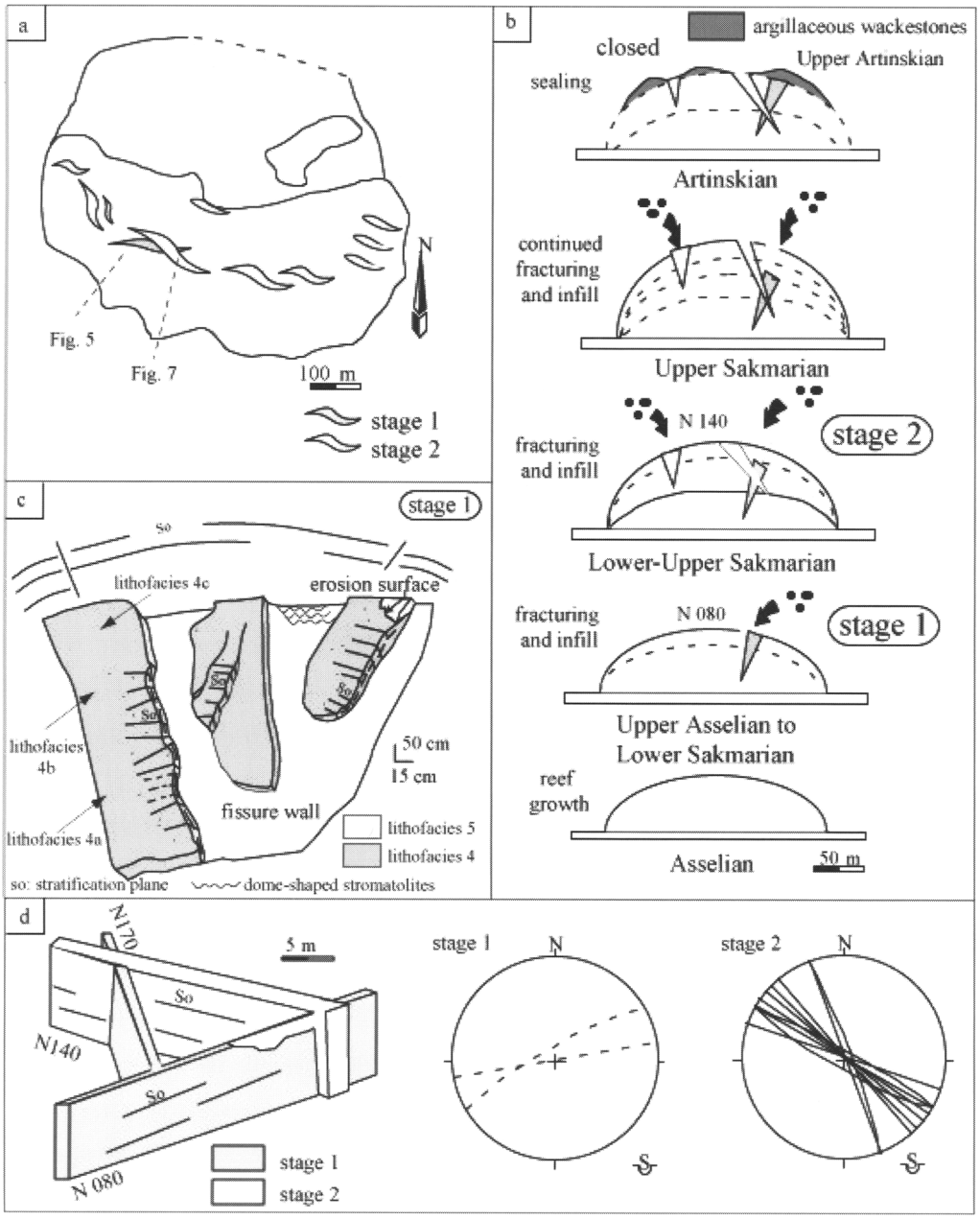


Fig. 5. (**a**) Representation of fractures cross-cutting the Tratau reef complex mainly observed in the well-exposed south flank of the reef. (**b**) Tectonically induced evolution of fractures: two-stage timing of dyke formation and stages of filling based on biostratigraphic data. (**c**) Schematic drawing illustrating a fracture opening and filling (stage 1, N80°; so, stratification). Lithofacies 4a – ooidal–peloidal packstones; lithofacies 4b – wackestones–packstones rich in gastropods; lithofacies 4c – micritic and peloidal wackestones with fenestral fabric; lithofacies 5 – packstones rich in echinoderms, underlying an erosion surface. (**d**) Simplified diagram showing Schmidt stereographic projections of planes of fissure walls. Two separate fracture assemblages have N80° and N130°–N140° orientations.

Downloaded from http://sp.lyellcollection.org/ at Carleton University Library on June 13, 2015

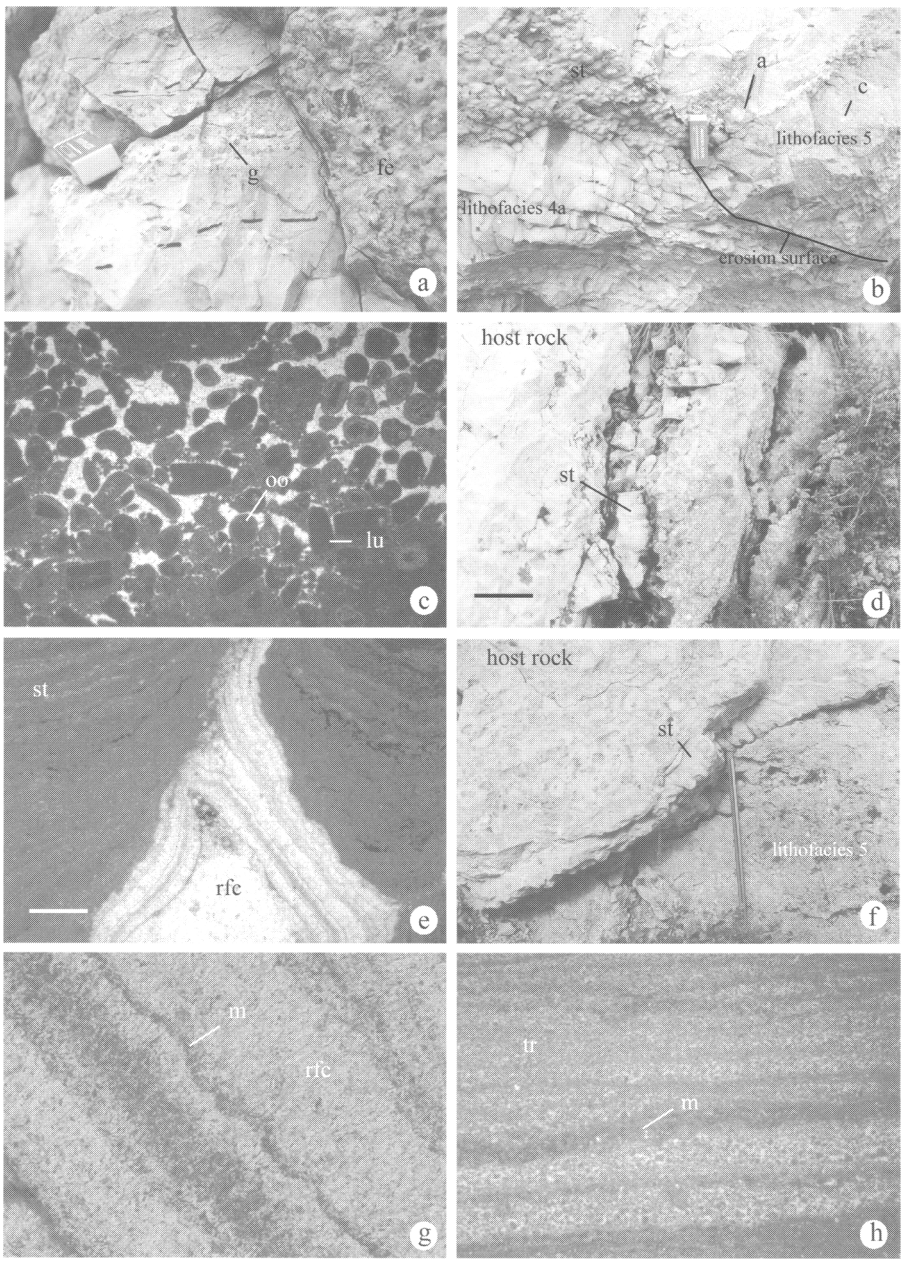


Fig. 6. (**a**) Neptunian dyke infilled with different lithofacies; ferrigeneous (fe), phosphatic crusts (lithofacies 1); stromatoid developed on dyke wall; gastropod-rich wackestone–packstone (lithofacies 4b). (**b**) Neptunian dyke (N80°) with complex infill: stromatoid encrusting the fracture wall (st); mudstone with fenestrae filled by fine dolomite (lithofacies 4c); erosion of the mudstone by crinoid-rich packstone (c), ammonoids (a) and other bioclasts (lithofacies 5). (**c**) Grainstone–packstone with ooids (oo) and lumps (lu); scale = 500 μm. (**d**) Neptunian dyke (fracture N140°) infilled with crinoid-rich packstone (lithofacies 5) and stromatoid (st) lining on the fracture wall; scale = 10 cm. (**e**) Dome-shaped microbial laminae (st, stromatoid) with depressions filled by radial fibrous cements (rfc); scale = 250 μm. (**f**) Neptunian dyke (N80°) infilled with encrinitic packstone (lithofacies 5); wall is encrusted by stromatoid crusts (st). (**g**) Radial fibrous cement layers (rfc) separated by thin dark microbial laminae (m); scale = 250 μm, top to the right. (**h**) Alternating grainstone layers with fibrous cements and peloidal packstones (tr); micritic dark layers seem microbial laminae (m, lithofacies 3); scale = 500 μm.

Downloaded from http://sp.lyellcollection.org/ at Carleton University Library on June 13, 2015

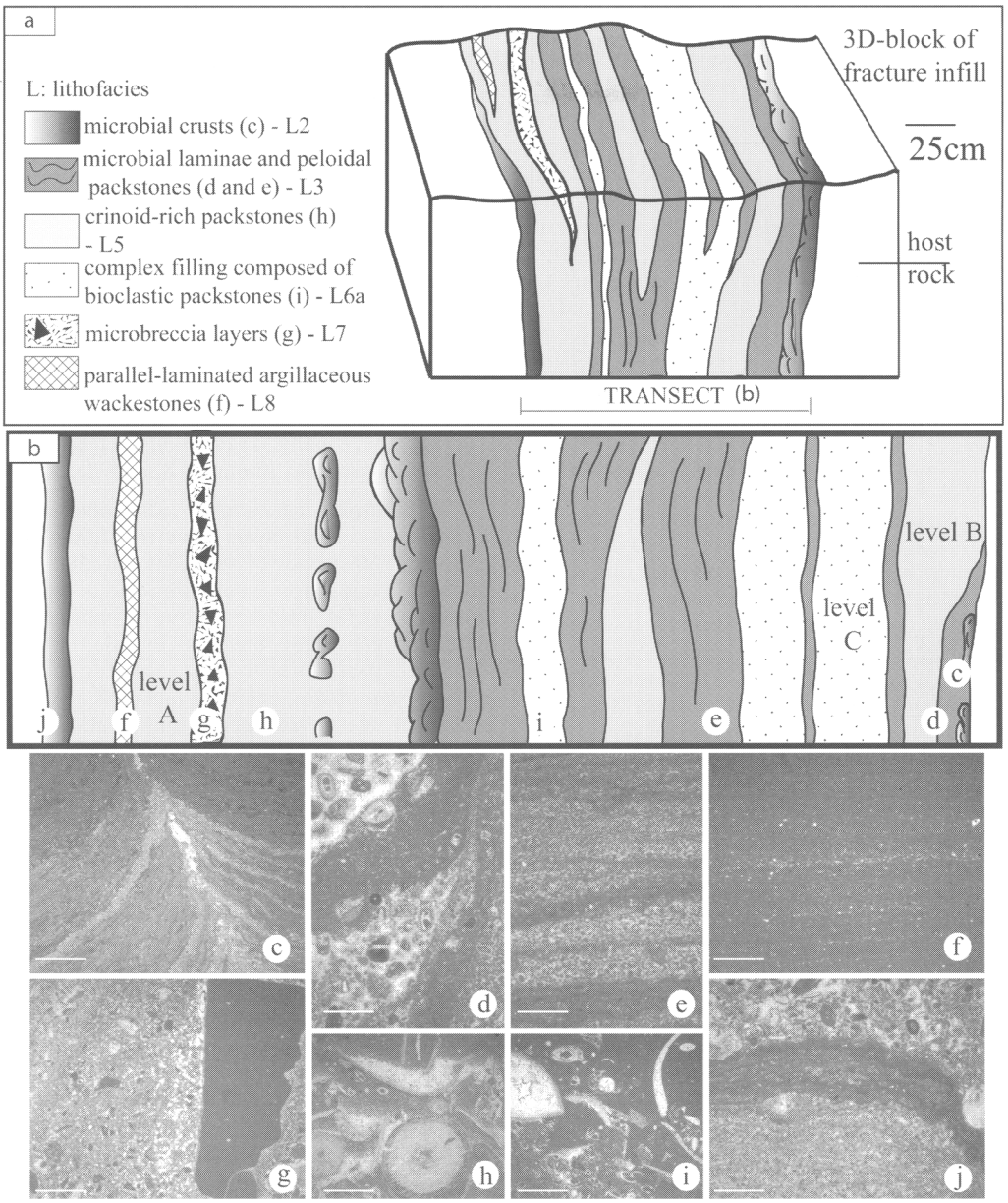


Fig. 7. (**a**) Three-dimensional diagram of fracture infill (fracture with N140° orientation) with opening and three dated episodes of synsedimentary filling: level A, crinoid-rich packstone: lower Tastubian (Sakmarian); level B, crinoid-rich packstone: upper Tastubian (Sakmarian); level C, bioclastic packstone: lower Sterlitamakian (Sakmarian). (**b**) Transect illustrating the main lithofacies distribution. (**c**) Stromatoid composed of dome-shaped microbial crusts (*Archeolithoporella*-like); scale = 500 μm. (**d**) Complex filling showing alternating bioclastic facies (lithofacies 6a), microbial laminae and peloids; scale = 500 μm. (**e**) Layers of peloids regular and homogeneous in size alternating with microbial laminae; scale = 500 μm. (**f**) Fine-grained argillaceous wackestones, laminae are perpendicular to the wall of dyke (lithofacies 8); scale = 500 μm. (**g**) Intraclastic sediments composed of angular lithoclasts embedded in a micritic–peloidal matrix (lithofacies 7); scale = 500 μm. (**h**) Crinoid-rich packstones (lithofacies 5); scale = 1 mm. (**i**) Bioclastic packstones with gastropods and fragmented bivalves and ostracods (lithofacies 6a); scale = 1 mm. (**j**) Contact between flanking bed and fracture wall, which is encrusted by microbial laminae.

Downloaded from http://sp.lyellcollection.org/ at Carleton University Library on June 13, 2015

ammonoids (lithofacies 5; Fig. 6b). Lithofacies 5 is dated as lower Sakmarian by conodonts (Chuvashov *et al.* 1996).

A first dyke episode took place shortly after the formation of the Tratau reef. This is evidenced by the fossil record of the dykes, which is different from the reef fabrics. The absence of taxa diagnostic of the reef growth and the relative abundance of gastropods and ostracods indicate reworking from an inner, protected reef setting or an autochthonous cryptic habitat in the fracture. Representatives of the dweller guild are the major constituents of the first fracture type. Gastropods and ostracods occur locally as dense clusters and are arranged together showing probably an *in situ* habitat with the organisms grazing on microbial matter. Members of the constructor and binder guilds are poorly represented because they were bound to the reef surface through encrustation and early cementation. Oolithic and lump layers (Fig. 6c) are not preserved in the sedimentary record of the reef and only occur in fractures. Therefore, these late Asselian relic sediments offer a good opportunity to complete the sedimentary succession, which is not preserved in the reef itself. The association of lithofacies 4c with emersive features (fenestrae, dissolution and dolomitization) at the top of the mud-dominated sedimentation permits the correlation of this episode with the late Asselian subaerial exposure evidenced throughout the East European platform by Aisenberg *et al.* (1983) and give information of the importance of the lowering of the relative sea level. Ages are based on the basis of the presence of ammonoids and conodonts (*Mesogondolella lacerta* and *Mesogondolella parafoliosa*) in the lithofacies 5 overlying the erosion surface observed in the greatest N80° dyke (Fig. 6b).

(ii) A multiple phase of layers parallel or inclined at low angles to the fracture walls appears in the second assemblage of fissures (N130°–N140° and N60°; Figs 6d & 7). This second type of tectonic-induced opening affects the previous fracturation and Asselian–Sakmarian host rocks. At least eight distinct neptunian lithofacies are recognized in some fractures. Some of them are recurring by repeated tectonically re-opening favouring development of vertical and steeply inclined walls. They present different ages from late Asselian to Artinskian (Fig.7). The arrangement of the lamination of the sediment-fill varies widely, from parallelism to obliquity and directly depends on the nature of the fill. Three phases of fracturing and infill may occur in a single fracture, indicating several stages in opening.

1. The opening of fissures began on a small-scale with microfracturing of a lithified host rock. Walls were lined with thin ferruginous and/or phosphatic crusts, or radial fibrous calcite cements (lithofacies 1).
2. Cracks were lined with alternating dome-shaped to microbial laminae and fibrous calcite cements (lithofacies 2, Figs 6e & 7c; lithofacies 3, Figs 6h & 7d, e).
3. Fissures opened into large, metre-scale dimensions, which were partially or completely filled with a late complex sediment succession (Fig. 7), composed of peloidal packstones (lithofacies 3), bioclastic packstones (lithofacies 5, Fig. 7h; lithofacies 6a and 6b, Fig. 7i), breccias (lithofacies 7, Fig. 7g) and, finally, argillaceous wackestones and claystones (lithofacies 8, Fig. 7f).

The multiple generations of sediments and the intercalated cement layers show that filling was episodic, with pulses of sediment injection and quiescent periods for cementation and microbial growth. Several fractures show an infill composed of polymictic breccias, included within bioclastic packstones–wackestones. Intraclasts, up to 50 cm in size, exhibit angular shapes and consist of internal sediments, microbialites and, sometimes, flanking bed fragments. The filling evidences episodes of tectonic instability by successive collapses of the fracture walls. The marine conditions of fissure infilling is indicated by the presence of: (i) foraminifers, gastropods, ostracods, conodonts and echinoderms in the fine-grained matrix; (ii) radial fibrous calcite cements between the clasts; and (iii) stable isotope values ($\delta^{18}O$ from −1 to −2‰ and $\delta^{13}C$ from 5 to 6‰) of radial fibrous calcite that show isotopic values similar to those recorded in subsurface and stromatactis.

The second fracture assemblage (N130°–N140°) probably formed during the lower Sakmarian based on their transections through the first fracture assemblage and the presence of *Mesogondolella lacerta* and *Mesogondolella parafoliosa* (level A, lower Tastubian, Sakmarian) in lithofacies 5, *Mesogondolella striata* and *Hindeodus* sp. (level B, upper Tastubian, Sakmarian) in the same lithofacies, and *Mesogondolella lata*, *Mesogondolella bisseli* and *Hindeodus* sp. in lithofacies 6a (bioclastic packstones, level C, lower Sterlitamakian, Sakmarian). The final infilling lithofacies 8 corresponds to the Artinskian indicated by the presence of ammonoids, foraminifers and orthoceratids (Rauser-Chernoussova 1951; Chuvashov *et al.* 1996).

Downloaded from http://sp.lyellcollection.org/ at Carleton University Library on June 13, 2015

Both fracture assemblages are similar in that: (i) thin ferrugineous, phosphatic crusts, dome-shaped microbialites and/or laminar layer of microbialites (lithofacies 2–3) directly line and encrust the wall of dykes. This indicates that the fractures remained for some time open before they were filled by external skeletal debris; (ii) a source from the surface is proposed for part of the filled sediment; and (iii) fissures disappear upwards and are overlain by upper Artinskian argillaceous wackestones.

They differ in that: (i) fractures exhibit different orientations; (ii) in the first fracture assemblage, lithoclasts of wall rock and cryptobiontic organisms evidence a passive sediment-fill by gravitational-induced processes; this contrasts with the injection processes from the second fracture type. The evidence for fracture-fill cementation and rebrecciation indicates that the process of fracture develop during several phases; (iii) the age of fracturing and filling is upper Asselian–lower Sakmarian for the first assemblage and upper Asselian–upper Artinskian for the second fracture assemblage. Lithofacies 5 (crinoidal packstones) is the last step of infilling for N80° fractures, and argillaceous wackestones and claystones are the last sediments for the N130°–N140° fractures.

Microbial texture

Fractures were cryptic habitats similar to those in the skeletal framework on the subsurface of the Permian reef of New Mexico (Wood *et al.* 1996). As in recent reef niches, marine microbialites are common structures in cavities and fractures (Reitner *et al.* 2000) and contribute to fracture filling as fixing and binding organisms. Microbial structures in the fractures are represented by stromatoid laminations, muddy matrix, clotted-peloidal fabrics (thromboid structures) and micritic laminae. Two general types of microbial fabrics are commonly recognized. (i) Up to 10 cm-thick stromatoid laminae appear planar–domical in shape, passing into clotted-like textures. Interdomal areas are filled by radial fibrous calcitic cements (Fig. 6e–g). They directly encrust fracture walls and synsedimentary re-opened fracture walls and act as pioneer organisms. They consist of dark micritic laminae. Organisms living in the fissures would be expected to be members of the Tratau framework communities as the problematic *Archaeolithoporella* and are observed in dykes and other cryptic sites of the Permian Capitan reef in Texas (Babcock 1977; Stanton & Pray 2004). *Archaeolithoporella* has been considered as alga (Mazzulo & Cys 1978; Wang *et al.* 1994; Kirkland *et al.* 1998), but Grotzinger & Knoll (1995) favour instead a microbialitic (Shen & Xu 2005) or organic-cement origin. It was apparently able to grow in very low light conditions as it is quite common in cryptic settings (Babcock 1979). In the Tratau reef *Archaeolithoporella* is frequently observed in association with stromatactis-like cavities; microbialitic structures in some fractures seem to be in good agreement with *Archaeolithoporella* structures (Sarfati pers. comm). *Archaeolithoporella* encrusted radial fibrous cements or distinctly grew between cements layers, suggesting that the cement was of syndepositional marine origin. Microbialites are repeatedly interlayered with radial fibrous calcite (Fig. 6g). Following Wahlman (1988), the relation between stromatolitic laminations and cements suggests that microbes might have played a role in the precipitation of 'botryoidal' macrocements but might also simply represent periodic cessations of 'botryoidal' cement growth. Occurrence of several generations of stromatolites in a single fracture points to various episodes of opening (Fig. 7). A sharp contact separates the stromatolites from the overlying laminated peloidal packstones and the thrombolitic facies (Figs 6f & 7b). The peloids in contact with stromatolitic layers present a mesoscopic clotted fabric. (ii) Thromboids correspond to unlaminated peloidal grainstones–packstones (Fig. 6h). They are frequently associated with millimetre-thick layers of fibrous cements and microbial laminae, which appear as amalgamated thin-layered micritic laminae and form a consortium with thromboids. They form flat to slightly undulating laminae. The thrombolitic facies is made of peloidal, clotted and homogeneous micrite (Fig. 6h). Peloids are well sorted and rounded, generally up to 100 μm in diameter and are composed of dark coloured micrite embedded in a groundmass of calcite microspar. Peloidal matrix grades into clotted and/or homogenous micrite. Wahlman (1988) proposed microbial activity as an origin for peloidal fabrics. Kirkland *et al.* (1988) proposed an *in situ* formation for the peloids within a mucilageneous organic film. Such 'peloidal sediments' have been described by Chafetz (1986) in modern carbonates as a product of microbially induced precipitation.

Discussion on regional tectonostratigraphic evolution and origin of fracturation

The north–south-trending area of transition between the eastern margin of the Russian platform and the preduralian basin is an excellent

Downloaded from http://sp.lyellcollection.org/ at Carleton University Library on June 13, 2015

area to study interacting structural and sedimentary processes. Orogenic collision was oblique, moving wave-like from south to north along the orogen (Puchkov 1997). Transverse NW–SE structural elements accommodated this oblique collision and subdivided the foreland into several semi-isolated basins. Tectonic processes in foreland basins have a clear 'first-order' control on the thickness of carbonate platform deposits and on its gross facies distribution (Jordan *et al.* 1988). The model of Palaeozoic collision in the Urals was complicated by the uneven outline of the passive margin, with a promontory in the middle Urals called the Ufimian amphitheatre (Puchkov 1997). In the Carboniferous, the southern Urals were characterized by an atypical collision and the formation of local tensional structures. During the Lower Permian a rigid collision followed, recording changes in intensity along the length of the orogen until the Late Permian (Puchkov 1997).

The origin and growth of reefs and associated fracturation were partly governed by synsedimentary tectonism, which is evidenced by: (i) the spotty distribution of reefs, the presence of regional north–south-trending faults, and the sharp variations in facies and thicknesses on flanks (Rauser-Chernoussova 1951); (ii) the widespread development of fault-bound depressions on the top of several reefs; (iii) the presence of synsedimentary fractures and neptunian dykes within reefs (Vennin 1997; Vennin *et al.* 2002). Four geodynamic phases in the development of Tratau and Shaktau reefs are proposed (Vennin *et al.* 2002): (i) reef growth began on tectonically induced palaeohighs during the Gzhelian; (ii) large isolated pinnacles are affected by fractures in the Asselian, as indicated by the age of the infilled sediments. After late Asselian karstification and erosion, the reef growth continued through the Sakmarian and early Artinskian ending by uplift and erosion; (iii) a tilting of the platform favoured the uplift of the entire Sterlitamak area during the early Artinskian (Vennin *et al.* 2002) and, at a local scale, explains the differential subsidence recorded by the Tratau and Shaktau reefs; (iv) finally, the platform and reefs were drowned during the late Artinskian because of siliciclastic influx related to thrusting and closure of the palaeo-Ural Ocean during the Artinskian (Zempolich *et al.* 2002).

Explanations for neptunian dyke formation are manifold. Some yield important information concerning the dyke formation in the Urals. Neptunian dykes crossing out in the Capitan reef carbonate margin are interpreted to have formed in response to differential compaction induced by the reef-loading of foreslope sediments (Yurewicz 1977; Jagnow 1979; Melim & Scholle 1991). Stanton & Pray (2004) proposed gravity settling and downwarping of lithified platform carbonate to explain neptunian dykes aligned parallel to the platform margin of the Capitan reef. A high local depositional relief and sediment instability can result in passive gravitational movement and fracturing of the rock. However, Hunt *et al.* (2002) argued that these fractures and faults were preferentially localized within the damage zones of syndepositional faults and not exactly related to the syndepositional down-to-the-basin tilting of the platform as proposed by Saller (1996). This latter process is a response to compaction-induced differential subsidence. The origin of neptunian dykes can also be related to tectonic mechanisms that cause fracturing or initiate gravitational movement (Cozzi 2000). Although the Lower Jurassic Hierlatzkalk dykes from Hungary are similar to those of the Capitan reef, their origin is attributed to normal faulting of the platform rather than to sedimentation-induced subsidence (Galacz 1998). Neogene intramontane basins of SE Spain have a complex structural history. Kinematic rearrangements during the Late Tortonian resulted in a significant tilting of blocks and formation of neptunian dykes (Brachert *et al.* 2001). Tectonic and seismicity at the southern Minervois margin (France) resulted in fault growth and formation of neptunian dykes in Emsian mound facies. The dykes formed during or immediately after mound accretion and simultaneously with cementation of the stromatactoid cavity networks (Bourrouilh *et al.* 1998). Fractures with synsedimentary filling occur also in the Late Frasnian 'Les Wayons' buildups of Belgium. Vertical extension-related fractures affected the mound facies, truncating and circumventing the fossils (Playford 1984; Boulvain 2001).

In the Tratau reef mound, small fissures connecting cavities and voids are attributed to passive gravitational movements but are only filled by fibrous radial cements. These fissures are systematically cut by the neptunian dykes described above. Explanations for tectonically induced origin of dykes invoke: (i) contemporaneous orthogonal dyke sets with an orientation corresponding to the regional tectonic fabric N90° and N80° (Rauser-Chernoussova 1951). Local tectonic events have been dated and integrated into a regional extensional tectonic episode, within a foredeep geodynamic model. The eastern margin of the Russian platform appears to have been governed from the Asselian

Downloaded from http://sp.lyellcollection.org/ at Carleton University Library on June 13, 2015

to the Artinskian by syndepositional movements on north–south-trending fault lines, parallel to the shelf edge. The formation of the fractures can be ascribed to differential movement between fracture-bounded blocks of host rocks resulting in dilation, or complete removal of blocks, presumably by gravitational mass movements. It is important to call attention to the paradox of contemporaneous normal faulting, subparallel to the strike of the reefbelt, and general compressional features in the eastern foreland. Distensional processes are recorded by the breakdown of the Lower Permian platform, and the common synsedimentary fractures and collapse structures recorded in the Tratau reef and in neighbouring reefal area (Shaktau). Winslow (1983) argued that dykes are restricted to the toe areas of thrust hanging walls. The same phenomena are also seen in the Alpine foldbelt (Laubscher 1978) and the Ouachita–Marathon forebelt (Hopkins 1968); (ii) the neptunian dykes cut the complete reef. They originated after lithification. This prevented a strictly passive gravitational-induced process affecting the reef flanks; and (iii) age of the neptunian sediment and their organization within the fractures are not consistent with a progressive opening of fractures towards the margin of the reef.

Conclusions

- Neptunian dykes filled with skeletal material are well developed and an abundant feature of the Tratau reef. As a result of a detailed study of the fractures affecting the Tratau reef, the following conclusions are drawn.
- Neptunian dykes provide insights concerning the reef biota and reef-growth episodes that are poorly preserved in subsurface. The dykes record fracture formation at the platform margin but represent orthogonal dyke sets with orientations corresponding to the regional tectonic fabric.
- Synsedimentary fissures and fractures, seen as neptunian dykes, are related to synsedimentary tectonism rather than gravitational phenomena on the reef flank. The formation of the neptunian dykes is related to the lower Asselian break-up (distensional period) of the reef connected to the orogenic evolution of the eastern foreland basin.
- Biostratigraphically diagnostic fossils in the dykes indicate that the fractures were formed from late Asselian to Artinskian time. The biostratigraphic analysis of the neptunian sediments indicates that there was a marked erosional gap (hiatus), spanning the Sakmarian–Early Artinskian on the Tratau reef surface. Argillaceous wackestones and claystones are the latest neptunian sediments. They are correlated with the late Artinskian drowning of the platform and the closure of the palaeo-Ural Ocean during the Artinskian.
- The fractures act as sediment traps for loose skeletal materials from the reef surface and act as niches for autochthonous biota (*Archaeolithoporella*, microbialites, rare ostracods and gastropods). Internal bioerosion is not observed on the walls, and bioclasts and endolitic biota seem to be absent. The framework reef communities are poorly preserved in the dykes because they were bound to the reef surface and thus were not a sediment source. Therefore, the dykes are filled by members of the vagile dweller and sessile binder (*Archaeolithoporella*) guilds. Fracture habitat was similar to the cryptic habitat within skeletal reef frameworks (as stromatactis-like cavities).
- The submarine origin of the filled fractures is evidenced by the consistent occurrence of marine sediments and marine calcite cements.

The author is grateful to H.-G. Herbig, B. Pratt and M. Aretz for helpful criticisms and suggestions, which have greatly improved this paper. I wish to express my thanks to all the scientists, Russian staff and Total Company who supported this research. This paper was improved by suggestions and comments made by B.I. Chuvashov (Institute of Geology and Geochemistry, Russia), B. Beauchamp (University of Calgary, Canada) and T. Boisseau (Total, France). D. Vachard (University of Lille, France) also contributed to improve the manuscript by his foraminifer determinations and M. Guiraud (University of Bourgogne, France) for his comments on tectonics.

References

AISENBERG, D. Y., POLETAYEV, V. I., MAKHLINA, M. K. & SHCHERBAKOV, O. A. 1983. Carboniferous sea level changes on the East-European platform. *X Congres International Stratigraphy Geology Carboniferous*, **4**, 65–71.

BABCOCK, J. A. 1977. Calcareous algae, organic boundstones, and the genesis of the upper Capitan Limestones (Permian, Guadalupian), Guadalupe Mountains, West Texas and New Mexico. *In*: HILEMAN, M. E. & MAZULLO, S. J. (eds) *Upper Guadalupian Facies, Permian Reef Complex, Gudalupe Mountains, New Mexico and West Texas.* Permian Basin Section, SEPM Field Conference Guidebook, Midland, Texas, **77–16**, 3–44.

BABCOCK, J. A. 1979. Calcareous algae and algal problematica of the Capitan reef (Permian), Guadalupe Mountains, West Texas and New Mexico, USA. *Bulletin des Centres de Recherches Exploration – Production Elf-Aquitaine*, **3**, 419–428.

Downloaded from http://sp.lyellcollection.org/ at Carleton University Library on June 13, 2015

BOULVAIN, F. 2001. Facies architecture and diagenesis of Belgian Late Frasnian carbonate mounds. *Sedimentary Geology*, **145**, 269–294.

BOURQUE, P. A. & BOULVAIN, F. 1993. A model for the origin and petrogenesis of the red stromatactis limestone of Paleozoic carbonate mounds. *Journal of Sedimentary Petrology*, **63**, 607–619.

BOURROUILH, R., BOURQUE, P. A., DANSEREAU, P., BOURROUILH-LE JAN, F. & WEYANT, P. 1998. Synsedimentary tectonics, mud-mounds and sea-level changes on a Paleozoic carbonate platform margin: a Devonian Montagne Noire example (France). *Sedimentary Geology*, **118**, 95–118.

BRACHERT, T. C., HULTZSCH, N., KNOERICH, A. C., KRAUTWURST, U. M. R. & STÜCKRAD, O. 2001. Climatic signatures in shallow-water carbonates: high-resolution stratigraphic markers in structurally controlled carbonate buildups (Late Miocene, southern Spain). *Palaeogeography, Palaeoclimatology, Palaeoecology*, **175**, 211–237.

CHAFETZ, H. S. 1986. Marine peloids: a product of bacterially induced precipitation of calcite. *Journal of Sedimentary Petrology*, **56**, 812–817.

CHUVASHOV, B. I. 1983. Permian reefs of the Urals. *Facies*, **8**, 191–212.

CHUVASHOV, B. I. 1984. *On Joint Line Between Russian Platform and Preduralyan Foredeep Metamorphism and Tectonic of Uralian Western Zones. Urals Scientific Centre of Academy of Sciences USSR Sverdlovsk*, 111–120.

CHUVASHOV, B., PROUST, J. N., BOISSEAU, T. & VENNIN, E. 1996. *On History of Development of Sterlitamakian Shikhans (Early Permian Reefs of Southern Preduralye). Proceedings of the Institute of Geology and Geochemistry*, **28**, 25–32 [in Russian].

COZZI, A. 2000. Synsedimentary tensional features in Upper Triassic shallow-water platform carbonates of the Carnian Prealps (northern Italy) and their importance as paleostress indicators. *Basin Research*, **12**, 133–146.

GALACZ, A. 1998. Tectonically controlled sedimentation in the Jurassic of the Bakony Mountains (Transdanubian Central Range, Hungary). *Acta Geologica Hungarica*, **31**, 313–328.

GERASIMOV, N. P. 1940. *Geology of the Eastern of Bearing Region (West Slope of the Urals and Western Preduralyde)*. Izdatelstvo, Academy of Sciences USSR, 1–140.

GROTZINGER, J. P. & KNOLL, A. H. 1995. Anomalous carbonate precipitates. Is the Precambrian the key to the Permian? *Palaios*, **10**, 578–596.

GUO, L. & RIDING, R., 1992. Aragonite laminae in hot water travertine crusts, Rapolano Terme, Italy. *Sedimentology*, **39**, 1067–1079.

HOPKINS, H. R. 1968. Structural interpretation of the Ouachita Mountains. *In*: CLINE, L. M. (ed.) *A Guide Book to the Geology of Western Arkoma Basin and Ouachita Mountains*. Oklahoma City Geological Society, 104–108.

HUNT, D. W., FITCHEN, W. M. & KOSA, E. 2002. Syndepositional formation of the Permian Capitan reef carbonate platform, Guadalupe Mountains, New Mexico, U.S.A. *Sedimentary Geology*, **154**, 89–126.

JAGNOW, D. H. 1979. *Cavern Development in the Guadalupe Mountains*. Cave Research Foundation, Columbus, OH.

JORDAN, J. E., FLEMINGS, P. B. & BEER, J. A. 1988. Dating thrust activity by use of foreland basin strata. *In*: PAOLA, C. & KLEINSPEHN, K. L. (eds) *New Perspectives in Basin Analysis*. Springer, New York, 307–330.

KIRKLAND, B. L., DICKSON, J. A. D., WOOD, R. A. & LAND, L. S. 1998. Microbialites and microstratigraphy: the origin of encrustations in the middle and upper Capitan Formation, Guadalupe Mountains, Texas and New Mexico, U.S.A. *Journal of Sedimentary Research*, **68**, 956–969.

KOROLYUK, I. K. 1985. *Methods and Results of the Study of the Permian 'Mt Shaktau' reef (Bashkirian section of the Western Urals)*. Moscow, Nauka. [in Russian].

LAUBSCHER, H. 1978. Foreland folding. *Tectonophysics*, **47**, 325–337.

LEES, A. 1964. The structure and origin of Waulsortian (Lower Carboniferous) reef of the West-central Eire. *Philosophical Transactions of the Royal Society of London*, **740**, 485–531.

MAZZULO, S. J. & CYS, J. M. 1978. *Archaeolithoporella*-boundstones and marine aragonite cements, Permian Capitan reef, New Mexico and Texas, USA. *Neues Jahrbuch für Geologie und Paläontologie, Monatshefte*, **10**, 600–611.

MELIM, L. A. & SCHOLLE, P. A. 1991. The fore reef facies of the Permian Capitan Formation: the role of sediment supply versus sea-level changes. *Journal of Sedimentary Research*, **65**, 107–118.

NALIVKIN, V. D. 1950. Fazii i geologichekaia istoria ufimskogo Plato i Juresano-Sylvenskoi. *Gostoptechizdat*, 1–127 [In Russian].

PLAYFORD, P. E. 1984. Platform-margin and marginal slope relationships in Devonian reef complexes of the Canning Basin. *Proceeding Geological Society Australia and Petroleum Exploration Society Australia Symposium Perth, Australia*, 190–214.

PUCHKOV, V. N. 1997. Structure and geodynamics of the Uralian orogen. *In*: BURG, J. P. & FORD, M. (eds) *Orogen through time*. Geological Society. Special Publication, **121**, 201–236.

RAUSER-CHERNOUSSOVA, D. M. 1951. Facies of Upper Carboniferous and Artinskian deposits in the Sterlitamak–Ishimbaevo region of the pre-Urals, based on a study of fusulinids. *Trudy Akademica Nauk SSSR, Series Geology*, **43**, 1–108 [in Russian].

REITNER, J., NEUWEILER, F. *ET AL.* 1995. Mud-mounds a polygenetic spectrum of fine-grained carbonate buildups. *Facies*, **32**, 1–69.

REITNER, J., THIEL, V., ZANKL, H., MICHAELIS, W., WÖRHEIDE, G. & GAUTRET, P. 2000. Organic and biogeochemical patterns in cryptic microbialites. *In*: RIDING, R. & AWRAMIK, S. M. (eds) *Microbial Sediments*. Spinger, Berlin, 149–159.

RIDING, R. 2000. Microbial carbonates: the geological record of calcified bacterial–algal mats and biofilms. *Sedimentology*, **47**, 179–214.

RIDING, R. 2002. Structure and composition of organic reefs and carbonate mud mounds: concepts and categories. *Earth-Science Reviews*, **58**, 163–231.

Downloaded from http://sp.lyellcollection.org/ at Carleton University Library on June 13, 2015

ROSS, C. A. & ROSS, J. R. P. 1990. Revised world maps. *In*: MCKERROW, W. S. & SCOTESE, C. R. (eds) *Paleozoic Paleogeography and Biogeography*. Geological Society, London, Memoirs, **12**, 1–21.

RUZHENCEV, V. E. 1956. *Early Permian Ammonoids of the Southern Urals. Ammonoids of Artinskian Stage.* Izdatelstvo, Academy of Sciences USSR, 1–275 [in Russian].

SALLER, A. H. 1996. Differential compaction and basinward tilting of the prograding Capitan reef complex, Permian, west Texas and southeast New Mexico, USA. *Sedimentary Geology*, **100**, 1–10.

SHAMOV, D. F. 1984. Faciès des dépôts sakmariens-artinskiens d'Ishimbaevskoe. *Travaux de l'Institut des Recherches pétrolières d'Oufa*, **2**, 3–77.

SHEN, J. W. & XU, H. L. 2005. Microbial carbonates as contributors to Upper Permian (Guadalupian-Lopingian) biostromes and reefs in carbonate platform margin setting, Ziyun County, South China. *Palaeogeography, Palaeoclimatology, Palaeoecology*, **218**, 217–238.

SLOSS, L. L. 1972. Synchrony of Phanerozoic sedimentary–tectonic events of the north American Craton and the Russian Platform. *24th International Geological Congress*, **6**, 24–32.

STANTON, R. J. & PRAY, L. C. 2004. Skeletal–carbonate neptunian dykes of the Permian Capitan reef, Texas, U.S.A. *Journal of Sedimentary Research*, **74**, 805–816.

VENNIN, E. 1997. *Architecture sédimentaire des bioconstructions Permo-Carbonifères de l'Oural méridional (Russie)*. Publications de la Société géologique du Nord, **26**.

VENNIN, E., BOISSEAU, T., PROUST, J. N. & CHUVASHOV, B. I. 2002. Influence of sea level change on reef architecture in Early Permian buildup complexes, southern Urals, Russia. *In*: ZEMPOLICH, W. G. & COOK, H. E. (eds) *Carbonate Reservoir and Carbonate Field Analogs.* Society of Paleontologists and Mineralogists, Special Publications, **74**, 205–218.

VISSARIONOVA, A. Y. A. 1975. *Field Excursion Guidebook for the Carboniferous Sections of the Urals (Bashkiria)*. Izdatelstvo Nauka, Moskva.

WAHLMAN, G. P. 1988. Subsurface Wolfcampian (Lower Permian) shelf margin reefs in the Permian basin of west Texas and southeastern New Mexico. *In*: MORGAN, W. A. & BABCOCK, J. A. (eds) *Permian Rocks of the Midcontinent*. Society of Paleontologists and Mineralogists, Midcontinent Section, Special Publications, **1**, 177–204.

WAHLMAN, G. P. & KONOVALOVA, M. V. 2002. Upper Carboniferous-Lower Permian Kozhim carbonate bank, Subpolar pre-Ural Mountains, northern Russia. *In*: ZEMPOLICH, W. G. & COOK, H. E. (eds) *Carbonate Reservoir and Carbonate Field Analogs.* Society of Paleontologists and Mineralogists, Special Publications, **74**, 219–241.

WANG, S. H., FAN, J. S. & RIGBY, J. K. 1994. The characteristics and development of the Permian reefs in Ziyun County, south Guizhou, China. *Acta Sedimentologica Sinica*, **14**, 66–74.

WEIDLICH, O. 2002. Middle–late Permian reef patterns. *In*: KIESSLING, W., FLÜGEL, E. & GOLONKA, J. (eds) *Phanerozoic Reef Patterns.* Society of Paleontologists and Mineralogists, Special publications, **72**, 339–390.

WEIDLICH, O. & FAGERSTROM, J. A. 1999. Influence of sea-level changes on development community structure, and quantitative composition of the upper Capitan massif (Permian) Guadalupe Mountains, Texas and New Mexico. *In*: SALLER, A. H., HARRIS, P. M., KIRKLAND, B. L. & MAZULLO, S. J. (eds) *Geologic Framework of the Capitan Reef*. Society of Paleontologists and Mineralogists, Special Publications, **65**, 139–160.

WINSLOW, M. A. 1983. Clastic dikes swarms and the structural evolution of the foreland fold and thrust belt of the Southern Andes. *Geological Society of America, Bulletin*, **94**, 1073–1080.

WINTERER, E. L. & SARTI, M. 1994. Neptunian dykes and associated features in southern Spain: mechanics of formation and tectonic implications. *Sedimentology*, **41**, 1109–1132.

WOOD, R., DICKSON, J. A. D. & KIRKLAND, B. L. 1996. New observations on the ecology of the Permian Capitan reef, Texas and New Mexico. *Palaeontology*, **39**, 733–762.

YUREWICZ, D. A. 1977. The origin of the massive facies of the lower and upper Capitan Limestone (Permian), Guadalupe Mountains, New Mexico and West Texas. *In*: HILEMAN, M. E. & MAZZULLO, S. J. (eds) *Upper Guadalupian Facies, Permian Reef Complex, Guadalupe Mountains, New Mexico and West Texas*. Permian Basin Section. SEPM Field Conference Guidebook, Midland, Texas, **77–16**, 45–92.

ZEMPOLICH, W. G. 1993. The drowning succession in Jurassic carbonates of the Venetian Alps, Italy: A record of supercontinent breakup, gradual eustatic rise, and eutrophication of shallow-water environments. *In*: LOUCKS, R. G. & SARG, J. F. (eds) *Carbonate Sequence Stratigraphy – Recent Developments and Applications*. AAPG, Memoirs, **57**, 63–105.

ZEMPOLICH, W. G., COOK, H. E. *ET AL.* 2002. The role of biotic and abiotic constituents in the development and diagenesis of middle to late Paleozoic carbonate platform: outcrops and subsurface examples from the C.I.S. *In*: ZEMPOLICH, W. G. & COOK, H. E. (eds) *Carbonate Reservoir and Carbonate Field Analogs.* Society of Paleontologists and Mineralogists, Special Publications, **74**, 123–180.

ZONENSHAIN, L. P., KORINEVSKY, V. G., KAZMIN, V. G., PECHERSKY, D. M., KHAIN, V. V. & MATVEENKOV, V. V. 1984. Plate tectonic model of the South Urals development. *Tectonophysics*, **109**, 95–135.